An Air-Stable Selenium/Zeolite Nanocomposite

Andreas Goldbach,*,† Lennox E. Iton,‡ Marcos Grimsditch,‡ and Marie-Louise Saboungi†

Centre de Recherche sur la Matière Divisée, Orléans, France, and Argonne National Laboratory, Argonne, Illinois

Received June 17, 2004. Revised Manuscript Received August 29, 2004

A novel selenium/faujasite nanocomposite was synthesized on the basis of Rb^+-exchanged zeolite Y. The confined selenium has an optical band gap of 2.62 eV and exhibits a significantly improved stability in air when compared to other selenium/faujasite composites. Its unique Raman spectrum consists of 12 well-resolved modes, which are attributed to Se_8 (D_{4d}) crowns and stable Rb^+ coordination complexes with this ring molecule. The Rb^+ coordination has a strong structure-directing effect on the confined Se, promoting a complete cyclization of the Se inside the cavities of zeolite Y. The extraordinary stability of this composite is credited to the matching dimensions of the Se_8 rings and the aluminosilicate framework as well as to the coordinative immobilization of the Se clusters.

Introduction

Encapsulation of clusters into molecular sieves is a versatile approach to study effects of confinement, since these hosts provide regular pore systems of nanoscopic dimensions and high-density cluster networks are readily generated. In particular, selenium/zeolite[1−10] and related II−VI semiconductor/zeolite[11−14] composites have been intensely studied in recent years because of the strong interest in nanostructured photoconductors and the technical importance of selenium. Up to now two structural motifs have been found when elemental Se was incorporated into molecular sieves. Sorption into aluminosilicates and aluminophosphates with one-dimensional channels, like mordenite or $AlPO_4$-5, resulted in the formation of isolated ordered Se chains,[3−6] while disordered chains prevailed in the wide open three-dimensional pore systems of faujasites (zeolites X and Y).[1−3,5,7,8] In some of these materials Se ring clusters were admixed as minor components. On the other hand, Se_8 and/or Se_{12} rings dominated in the smaller pore systems of zeolite A,[1−3,5] and only Se_6 rings were found in the electroneutral SiO_2 matrix decadodecasil 3R (DDR).[9]

A common characteristic of small Se clusters trapped inside molecular sieves is the remarkably good agreement of their Raman spectra with those of freely moving molecules, which suggests fairly weak interactions with the host matrices. So far significant electronic coupling between confined Se and zeolite matrices has been mainly observed when the latter contained transition-metal cations with open d-shells,[4,15] but the weaker interaction with non-transition-metal cations contributes also to the stability of these composites[16] and influences the equilibrium between Se chains and rings in zeolite Y.[8] However, no direct evidence has been presented yet for stable bonding of Se clusters to non-transition-metal cations inside molecular sieves. In the past we studied the behavior of Se in zeolite Y in the presence of alkaline earth, rare earth, and transition-metal ions.[17] Two early investigations of Se confined in Na−Y reported the formation of Se chains.[2,3] We turn our attention now to the confinement of Se within the Rb^+-exchanged form, because we previously observed an increased tendency to Se cyclization upon confinement of the chalcogen in Sr^{2+}-exchanged zeolite Y.[8] The Rb^+ ion is isoelectronic with Sr^{2+}, and Rb^+ could have a similar structure-directing effect on Se as suggested by a recently discovered crystalline polyselenide,

* Corresponding author. E-mail: goldbach@cnrs-orleans.fr.
† Centre de Recherche sur la Matière Divisée.
‡ Argonne National Laboratory.

(1) Bogomolov, V. N.; Lutsenko, E. L.; Petranovskii, V. P.; Kholodkevich, S. V. *JETP Lett.* **1976**, *23*, 482.
(2) Terasaki, O.; Yamazaki, K.; Thomas, J. M.; Oshuna, T.; Watanabe, D.; Sanders, J. V.; Barry, J. C. *Nature* **1987**, *330*, 58.
(3) Parise, J. B.; MacDougall, J. E.; Herron, N.; Farlee, R.; Sleight, A. W.; Wang, Y.; Bein, T.; Moller, K.; Moroney, L. M. *Inorg. Chem.* **1988**, *27*, 221.
(4) Endo, H.; Inui, M.; Yao, M.; Tamura, K.; Hoshino, H.; Katayama, Y.; Maruyama, K. *Z. Phys. Chem. Neue Folge* **1988**, *156*, 507.
(5) Poborchii, V. V.; Ivanova, M. S.; Petranovskii, V. P.; Barnakov, Yu. A.; Kasuya, A.; Nishina, Y. *Mater. Sci. Eng. A* **1996**, *217−218*, 129.
(6) Tang, Z. K.; Loy, M. M. T.; Goto, T.; Chen, J.; Xu, R. *Solid State Commun.* **1997**, *101*, 333.
(7) Armand, P.; Saboungi, M.-L.; Price, D. L.; Iton, L.; Cramer, C.; Grimsditch, M. *Phys. Rev. Lett.* **1997**, *71*, 2061.
(8) Goldbach, A.; Iton, L.; Saboungi, M.-L. *Chem. Phys. Lett.* **1997**, *281*, 69.
(9) Wirnsberger, G.; Fritzer, H. P.; Zink, R.; Popitsch, A.; Pillep B.; Behrens, P. *J. Phys. Chem. B* **1999**, *103*, 5797.
(10) Bichara, C.; Raty, J. Y.; Pellenq, R. J.-M. *Phys. Rev. Lett.* **2002**, *89*, 016101.
(11) Moller, K.; Eddy, M. M.; Stucky, G. D.; Herron, N.; Bein, T. *J. Am. Chem. Soc.* **1989**, *111*, 2564.
(12) Ozin, G. A.; Steele, M. R.; Holmes, A. J. *Chem. Mater.* **1994**, *6*, 999.
(13) Brigham, E. S.; Weisbecker, C. S.; Rudzinski, W. E.; Mallouk, T. E. *Chem. Mater.* **1996**, *8*, 2121.
(14) Brühwiler, D.; Leiggener, C.; Claus, S.; Calzaferri, G. *J. Phys. Chem. B* **2002**, *106*, 3770.
(15) Goldbach, A.; Saboungi, M.-L.; Iton, L.; Price, D. L. *J. Chem. Phys.* **2001**, *115*, 11254.
(16) Goldbach, A.; Saboungi, M.-L.; Iton, L.; Price, D. L. *J. Chem. Soc., Chem. Commun.* **1999**, 997.
(17) Goldbach, A.; Saboungi, M.-L. *Eur. Phys. J. E* **2003**, *12*, 185.

10.1021/cm049030h CCC: $27.50
Published on Web 11/03/2004

$Rb_2[Pd(Se_4)_2]\cdot Se_8$, which features a previously unknown crown ether-like coordination of Rb^+ ions by Se_8 rings.[18]

In the following we present Raman spectroscopic and diffuse reflectance results of the novel Rb−Y·10Se nanocomposite. Raman spectroscopy is widely used in the study of these host−guest compounds, since the crystallographic analysis of the confined selenium is complicated due to disorder effects.[1,4−9] In particular, we studied the stability of this material in air and compared the behavior in air to that of a selenium/zeolite Y composite that contains Ca^{2+} instead of Rb^+ ions.

Experimental Section

A commercial Na−Y zeolite (SigmaAldrich) was twice ion-exchanged with an aqueous $RbNO_3$ solution, heated under vacuum to 550 °C, treated with oxygen, and finally calcined in a vacuum at that temperature for 24 h. Chemical analysis yielded $Na_{10.5}Rb_{44}Al_{54.5}Si_{137.5}O_{384}$ (Rb−Y), indicating 80% ion exchange. The dehydrated zeolite was transferred to an Ar-filled glovebox, where calculated amounts of Rb−Y and Se were loaded into the two arms of a quartz U-tube, separated by a frit, to introduce 10 Se atoms per faujasite supercage. After sealing-off the tube under vacuum ($P < 5\cdot10^{-4}$ Torr) it was heated to 350 °C for 1 week. The Se was fully taken up by the zeolite to yield a brightly orange powder of nominal composition $Na_{10.5}Rb_{44}Al_{54.5}Si_{137.5}O_{384}\cdot 80Se$ (Rb−Y·10Se).

The setup for the Raman measurements consisted of a triple Jobin Yvon T64000 spectrometer equipped with an optical multichannel analyzer. Multiple lines in the visible range of a krypton ion laser were used for excitation: 476.2, 530.9, 568.2, 647.1, and 752.5 nm. The resolution of the instrument was 3 cm^{-1} at 647.1 nm, and samples vacuum-sealed in quartz tubes were used for the measurements. The spectra have been normalized by the usual Bose factor to correct for the temperature dependence of the measured intensities: $I = I_0[1 - \exp(-h\nu/k_BT)]$, $T = 300$ K.

A Varian Cary 5 spectrophotometer equipped with a Harrick Praying Mantis accessory was used to measure the diffuse reflectance R_∞ of the Rb−Y·10Se using magnesium oxide and the pure zeolite as reference materials. The samples were loaded inside a drybox into the airtight sample cell. The measured reflectance spectra were converted into Kubelka−Munk functions $F(R_\infty)$,[19] which represent the ratio of absorption coefficient α and scattering coefficient s: $F(R_\infty) = (1 - R_\infty)^2/2R_\infty = \alpha/s$. We show the Kubelka−Munk functions in the following since they agree reasonably well with the absorbance in the spectral range of interest here, because the scattering coefficient s of zeolites are almost constant over the range.

Results

Figure 1 shows the Raman spectra of Rb−Y zeolite before and after loading with Se. The spectrum of the pristine Rb−Y is in excellent agreement with that of the literature.[20] The zeolite framework bands make only minor contributions to the spectrum of the Se-loaded zeolite, which is consistent with previous studies on Se confined in zeolites.[17,21] The main framework band at 294 cm^{-1} is observed and the bands at 64 and 79 cm^{-1} are close to framework bands of the pristine zeolite as well. The Rb−Y·10Se spectrum differs markedly from

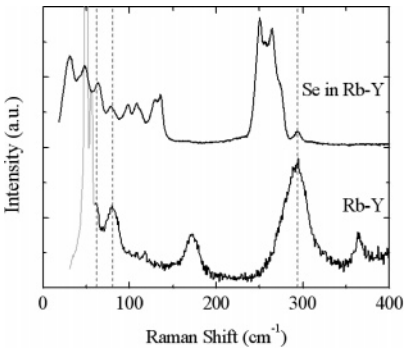

Figure 1. The Raman spectra of zeolite Rb−Y (excited at 568 nm) and the Rb−Y·10Se nanocomposite (excited at 752 nm). The dotted lines mark the positions of zeolite framework modes that could contribute to the spectrum of the composite. Laser plasma lines at 568 nm conceal the low-frequency range of Rb−Y.

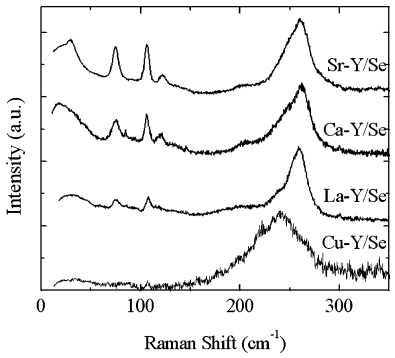

Figure 2. Raman spectra of selenium/zeolite Y nanocomposites with varying zeolitic countercations.[17]

other Se/zeolite Y nanocomposites (Figure 2).[17] The narrow bands split into a low-frequency group below 150 cm^{-1} and a high-frequency group between 230 and 300 cm^{-1} (Figure 1), pointing to well-defined Se structures. In contrast, very broad Raman bands indicate disordered Se chains in zeolites (Figure 2). Those contribute only as weak background to the spectrum of Rb−Y·10Se. Ordered chains and short chain fragments can be excluded on the basis of known Raman spectra[22,23] leaving Se rings as the most-likely alternatives. For instance, Se_8 molecules in Sr−Y zeolite are associated with narrow bands at 30, 75, 107, and 122 cm^{-1} (Figure 2).[8]

Cyclic structures are the most stable selenium clusters with more than five atoms.[24] Raman spectra have been reported for zeolite-confined Se_6,[9] Se_8,[8] and Se_{12} rings,[5] but these are less complex than the spectrum displayed in Figure 1. Thus, the large number of bands could be a signature of more than one Se species. Consequently, we probed the energy dependence of the Rb−Y·10Se spectrum to ascertain whether differences in the relative band intensities appear. Figure 3 shows Raman spectra measured at different excitation wavelengths. The optical band gap of the confined Se is larger than 2.5 eV according to standard evaluation procedures (vide infra), but the optical density of the confined

(18) Wachhold, M.; Kanatzidis, M. G. *J. Am. Chem. Soc.* **1999**, *121*, 4189.
(19) Kortüm, G. *Reflectance Spectroscopy*; Springer: New York, 1969.
(20) Brémard, C.; Le Maire, M. *J. Phys. Chem.* **1993**, *97*, 9695.
(21) Raman spectroscopy is relatively more sensitive to the confined selenium than to the aluminosilicalite framework due to the much larger polarizability of selenium.
(22) Mooradian, A.; Wright, G. B. In *The Physics of Selenium and Tellurium*; Cooper, W. Ch., Ed.; Pergamon: Oxford, 1969; p 269.
(23) Kohara, S.; Goldbach, A.; Koura, N.; Saboungi, M.-L.; Curtiss, L. A. *Chem. Phys. Lett.* **1998**, *287*, 282.
(24) Becker, J.; Rademann, K.; Hensel, F. *Z. Phys. Chem.* **1991**, *173*, 21.

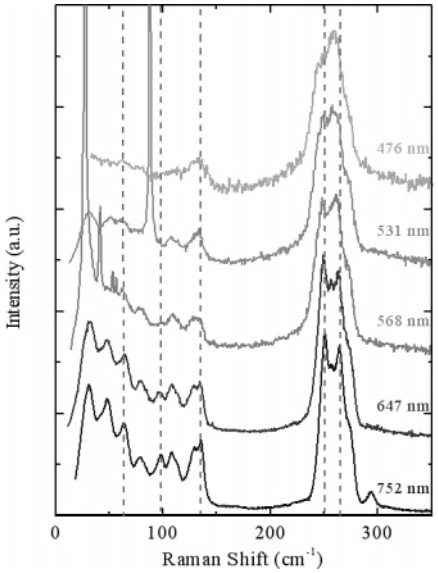

Figure 3. The Raman spectrum of Rb−Y·10Se at different excitation wavelengths. The dashed lines mark bands that decrease disproportionately as the laser is tuned through the visible spectral range. At 531 and 568 nm the low-frequency bands are obscured through laser plasma lines.

selenium increases already at 1.8 eV (i.e., $\lambda < 700$ nm) appreciably. This and the lower instrumental resolution at shorter wavelengths lead to a blurring of the Raman bands as the excitation energy is increased. Still, some trends can be recognized. The band at 294 cm^{-1} is only visible for excitation with 752 nm, while the bands at 64 and 79 cm^{-1} gradually decrease as the excitation energy rises. This suggests that only the 294 cm^{-1} band originates from the aluminosilicate framework and that all intrinsic zeolite modes are concealed at higher excitation energies due to resonant enhancement of the Se-related modes. The low-frequency bands fade increasingly as the laser is tuned from red to blue, while the high-frequency bands become increasingly less well resolved. Yet, it is evident that the two prominent bands at 250 and 263 cm^{-1} decrease relative to the one at 259 cm^{-1}, and that those at 98 and 136 cm^{-1} diminish in comparison to their neighbors as well. Thus, these four vibrational modes are distinct from those at 79, 109, 130, 259, and 272 cm^{-1}. The bands below 70 cm^{-1} also diminish nonuniformly in intensity with decreasing excitation wavelength, but strong laser plasma lines at 568 and 531 nm prohibit the consistent assessment of relative intensity variations of individual bands. Nevertheless, the differential response of the bands to changes in the excitation wavelength indicates that at least two Se species occupy the cages of the zeolite framework. One set of Raman bands can be identified with Se_8 (D_{4d}) crowns, as evidenced in Table 1, where we compare calculated vibrational modes of this crown-shaped molecule[23,25] with the spectrum of Rb−Y·10Se. The agreement between the bands attributed to Se_8 in Rb−Y and the calculated single molecule Raman spectrum is remarkably good considering the strong electrostatic fields and the spatial constraints within the zeolite pores. This suggests that the conformation of Se_8 inside the Rb−Y supercage is close to the ideal D_{4d} symmetry. Only the mode at 130 cm^{-1} deviates by ca. 10% from the corresponding calculated value of 116 cm^{-1}, possibly due to particular restriction of the related bending motion within the Rb^+-filled supercage. For comparison, this mode appears at 128 cm^{-1} in the Raman spectrum of monoclinic selenium (m-Se), where the integration of the Se_8 crowns into a crystal lattice leads to a restriction of bending motions, as indicated by the generally blue-shifted low-frequency modes.[23,26] The remaining bands of the Rb−Y·10Se at 48, 64, 98, 136, 250, and 263 cm^{-1}, however, cannot be reasonably attributed to any known molecular Se cluster on the basis of the available ab initio quantum chemical calculations or experimental data.

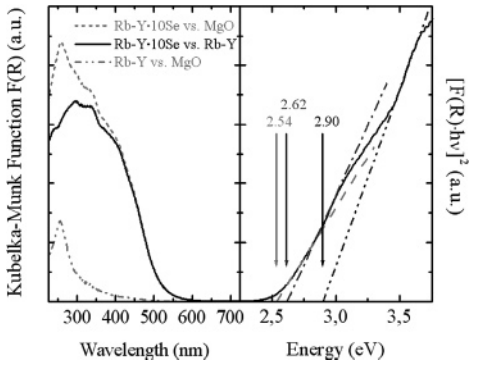

Figure 4. (a) Room temperature optical behavior of Rb−Y (dash dotted) and Rb−Y·10Se (dotted) with MgO as reference and of the confined selenium (solid line); (b) direct band gaps of the confined selenium determined from the energy dependence of the absorbance at the onset of absorption.

Table 1. Raman Frequencies (cm^{-1}) of Rb−Y·10Se and Calculated Vibrational Modes of Se_8 (D_{4d})[23,25]

frequencies of Rb−Y·10Se (cm^{-1})	calculated Se_8 modes		
	frequency	symmetry	activity
31	32	E_2	Raman
48			
64			
79	77	E_2	Raman
	95	E_1	IR
98			
109	106	A_1	Raman
130	116	E_3	Raman
	122	B_2	IR
136			
250			
259	259	A_1	Raman
	261	E_1	IR
263			
272 (sh)	274	E_2	Raman
	276	E_3	Raman
	275	B_1	inactive
294 (zeolite)			

Figure 4a shows the Kubelka−Munk functions of Rb−Y and Rb−Y·10Se with MgO as reference (under Ar). The electronic band around 255 nm in the pure zeolite is possibly due to an impurity. Since we were primarily interested in the optical properties of the confined selenium, we used the pure zeolite as reference to determine the electronic spectrum of the selenium/Rb−Y composite. The optical density of the confined selenium increases rapidly below 500 nm, reaching a

(25) A scaling of the calculated frequencies from ref 23 by a factor 0.85 appears to be more appropriate than using 0.893 as indicated in ref 23 when comparing them with Raman spectra of Se clusters confined in molecular sieves (see also ref 8).

(26) Lucovsky, G.; Mooradian, A.; Taylor, W.; Wright, G. B.; Keezer, R. C. *Solid State Commun.* **1967**, *5*, 113.

double maximum at 295 and 340 nm. On the low-energy side, a second electronic transition appears around 400 nm, and a further electronic band emerges as a very weak shoulder around 450 nm. The two lowest dipole-allowed B_2 and E_1 transitions of bulk m-Se are centered at 3.2 eV (390 nm) and 4.2 eV (295 nm),[27] which agree well with the strong shoulder and the second maximum observed in the absorption spectrum of the confined selenium. It is known that the UV/vis spectra of molecular solids such as m-Se correspond to those of the single molecules, except for some broadening and sometimes a shift in the solid state.[28] It is therefore not surprising to find very similar absorption bands in a molecular nanocomposite containing Se_8. Monoclinic selenium exhibits a direct band gap, which means that the square of the product $[F(R_\infty)\cdot h\nu]$ scales linearly with energy $h\nu$ at the absorption onset.[29] The corresponding plot in Figure 4b yields a band gap of 2.54 eV, practically identical with that of m-Se (2.53 eV).[30] However, this band gap is linked to the weak electronic band above 450 nm. The leading edges of the two dominant electronic bands around 400 and 340/295 nm were extrapolated too, as shown in Figure 4b, because they are more characteristic for this composite, as will be seen below. We obtained 2.62 and 2.90 eV, respectively, for the onsets of these transitions.

Se/zeolite Y composites are in general air sensitive and all manipulations have to be carried out in inert atmospheres. For instance, for diffuse reflectance measurements, the samples were loaded inside a glovebox into an airtight accessory of the spectrometer. However, when we exposed Rb−Y·10Se to air, we noticed that unlike other Se/zeolite Y composites the color of this one did not change, even after a few days. Intrigued by this observation, we monitored the optical properties in air as a function of time. Figure 5 compares the Ar-protected composite with that exposed for 10 and 30 days to air. The absorption threshold shifts increasingly to the red with time due to broadening of the leading weak absorption band, but the main electronic transitions in the visible and the near-UV remain unchanged. In fact, the onset of the first main transition is still at 2.62 eV, while the direct band gap decreased to 2.46 eV. For comparison, we show also spectra of Se confined in Ca^{2+}-exchanged zeolite Y. This composite contains mainly Se chains and only few Se_8 molecules (Figure 2). Within 2 days the appearance and the absorption spectrum of that material changed entirely. Two new strong electronic bands appear at lower energies and the absorption edge is significantly shifted as well. Further exposure to air leads only to relatively small intensity gains of the new features. The direct band gap obtained after 20 days in air is 2.08 eV with an initial value of 2.70 eV. The reduced band gap compares with those of trigonal Se (t-Se) (1.95 eV) and amorphous Se (a-Se) (2.05 eV),[29,31] which consist of ordered and disordered Se chains, respectively. The formation of amorphous/trigonal Se was confirmed by the Raman spectrum of the air-exposed Ca−Y·12Se (Figure 6b), which showed the characteristic narrow 233 cm^{-1} band of t-Se and the much broader 250 cm^{-1} band of a-Se[26,32] but no traces of the original spectrum of that nanocomposite (Figure 6a). In stark contrast, the Raman spectrum of Rb−Y·10Se retained its general features even after 30 days of air exposure with only minor t-Se and a-Se degradation bands (Figure 6d). We note that the broad 250 cm^{-1} band of a-Se coincides with the narrower Rb−Y·10Se bands in that range and enhances them disproportionately relative to the other bands of the

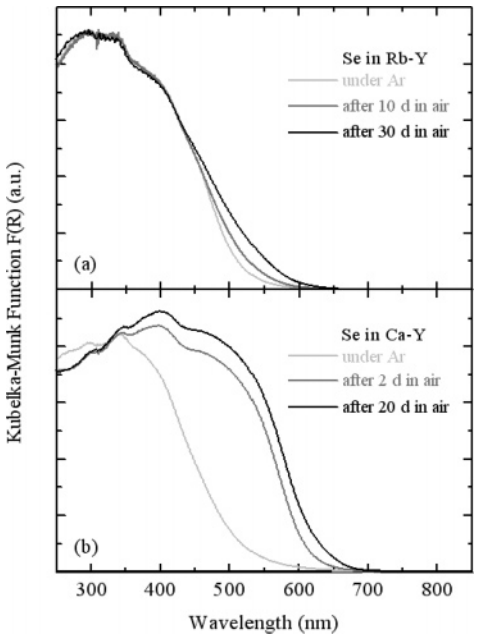

Figure 5. Optical behavior of (a) Rb−Y·10Se and (b) Ca−Y·12Se as function of time in air.

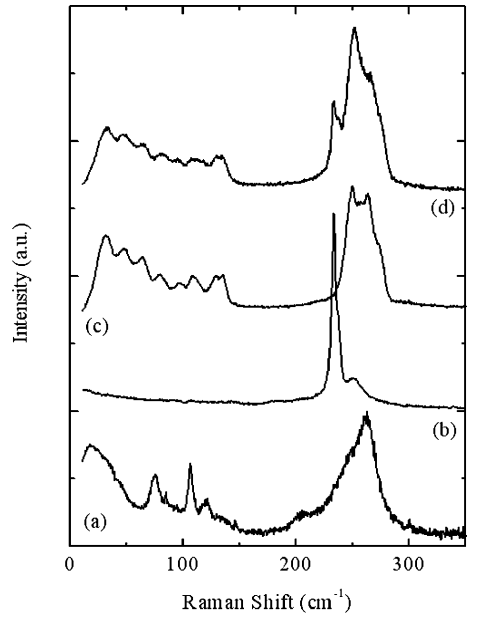

Figure 6. Raman spectra of Ca−Y·12Se (a) sealed under vacuum and (b) after 20 days in air and of Rb−Y·10Se (c) sealed under vacuum and (d) after 30 days in air.

(27) Dalrymple, R. J. F.; Spear, W. E. *J. Phys. Chem. Solids* **1972**, *33*, 1071.
(28) Salaneck, W. R.; Duke, C. B.; Paton, A.; Griffiths, C.; Keezer, R. C. *Phys. Rev. B* **1977**, *15*, 1100.
(29) Mott, N. F.; Davis, E. A. *Electronic Processes in Noncrystalline Semiconductors*; Clarendon, Oxford, 1979.
(30) Knights, J. C.; Davis, E. A. *Solid State Commun.* **1972**, *11*, 543.
(31) Goldbach, A.; Saboungi, M.-L. *Ber. Bunsen-Ges. Phys. Chem.* **1997**, *101*, 1660.
(32) The released Se on the surface is initially amorphous-like, but it rapidly transforms into trigonal Se under 647-nm laser radiation.

composite. The continuous scattering of a-Se below 150 cm^{-1} leads likewise to a smearing out of the Rb−Y·10Se bands in that region. The Raman spectrum of the Rb−Y·10Se exposed to air is therefore still dominated by the composite bands, in full agreement with the optical spectrum displayed in Figure 5a.

Discussion

The Raman spectra of the air-exposed materials indicate that Se chains migrate out the Ca−Y cavities. This happens only to a minor extent when Rb−Y·10Se is exposed to air, which corroborates our conclusion that chains play an insignificant role in this composite. The conversion of the confined Se clusters into chains is very slow at room temperature. The weak low-energy electronic transition of Rb−Y·10Se, which broadens upon air exposure, is attributed to the small amount of chains, while the dominant electronic bands at higher energy characterize the predominant ring clusters. Electronic bands with an onset around 2.90 eV were previously attributed to Se_8 in Sr−Y.[31] The transition characterized by the 2.62 eV onset could be due to the not yet identified Se clusters.

It appears that the oxygen does not destabilize the Ca−Y selenium composite in air, since no Raman bands due to oxidized Se species are found after air exposure. Hence, it is probable that the moisture is initiating the degradation. We have previously shown that Se−cation interactions within the supercage are important for the stability of composites holding mainly Se chains.[16] Water molecules likely enter the zeolite pores and displace the chains from the cations, which then become very mobile and migrate to the surface, where they form amorphous-like layers. The unusual stability of Rb−Y·10Se to air can be related to the total cyclization of the confined Se. For example, the diameter of Se_8 (D_{4d}) is close to the width of the windows (7.5 Å) interconnecting the supercages[33] and diffusion of these rings within the pore system should be very slow. In contrast, Se chains could readily slide through the 7.5 Å apertures, even when cations reside in there, because they have a much smaller kinetic diameter on the order of the van der Waals diameter of atomic Se, i.e., ca. 4 Å.[34] Yet Se chains are practically absent in Rb−Y, which contrasts markedly with other known Se/faujasite composites. This includes Y zeolites with monovalent, divalent, and trivalent cations,[3,7,8,15−17] and Na−X zeolite, which also stabilizes Se chains.[1−3,5] Since the presence of Rb^+ ions is the unique feature of the Rb−Y·10Se composite, we propose that interactions with the Rb^+ ions are responsible for shifting the equilibrium entirely to rings.

The coordination of covalent selenium clusters to alkali metal ions is a new form of complexation chemistry that has not been directly observed in zeolite cages before. Se_8 can form very stable coordination complexes with Rb^+ ions, as has been recently discovered.[18] The polyselenide $Rb_2[Pd(Se_4)_2]\cdot Se_8$ includes infinite $[Rb(Se_8)]_x^{x+}$ columns running through polymeric $[Pd(Se_4)_2]_x^{2x-}$ sheet anions with Rb^+ ions coordinated to Se_8 rings in a crown ether-like fashion.[18] A second type of Rb^+ ions coordinates edge-on to four Se_8 rings within the planes that the latter form between the $[Pd(Se_4)_2]_x^{2x-}$ sheet anion layers. A tetrahedral coordination of Rb^+ by Se_6 rings has been observed in $Rb_3AsSe_4\cdot 2Se_6$.[35] Equivalent complexes of other alkali metal ions with Se rings are not yet known, but Cs^+ ions form crown ether-like coordination complexes with Te_8 rings: $[Cs(Te_8)]_x^{x+}$ columns are found in Cs_4Te_{28}, while Cs_3Te_{22} includes $[Cs(Te_8)_2]^+$ clusters.[36,37] Apparently highly specific affinities exist between certain alkali metal ions and chalcogens, which can stabilize chalcogen rings even under unusual circumstances. For example, differential thermal analysis of $Rb_2[Pd(Se_4)_2]\cdot Se_8$ revealed that Se_8 rings survive in the melt up to 280 °C in the presence of Rb^+ ions,[18] while monoclinic Se_8 transforms into t-Se (helical chains) at 155 °C.[34] On the other hand, a bulk tellurium phase corresponding to monoclinic selenium (Se_8) is not known,[34] which indicates that coordination to Cs^+ is essential for the stabilization of Te_8 rings.[36,37] Hence, it is plausible to argue that Rb^+ exerts a structure-directing effect on Se confined in zeolites.

We propose that Rb^+ ions in zeolite Y shift the equilibrium between Se chains and Se_8 via complexation of the rings as they are formed. There are two types of cation sites in the supercage of zeolite Y, one near the 6-ring windows opening into the small sodalite cages (site II) and the other near the 4-rings in the large windows connecting adjacent supercages (site III).[33] Most likely the Se_8 rings bind to the loosely bound Rb^+ ions in site III at the Se sorption temperature. Two studies have addressed the distribution of Rb^+ ions in dehydrated Rb−Y zeolites as determined by Rietveld refinement of high-resolution synchrotron X-ray diffraction (XRD) patterns. Marra et al.[38] did not find any cations in the large windows of $Na_{21}Rb_{29}Al_{52.4}Si_{139.6}O_{384}$ (58% Rb^+-exchanged) at room temperature, which is similar to the fully Na^+-exchanged form, but that finding might be attributable to the low level of exchange. Ciraolo et al.[39] located 10.4 Na^+ and 47.2 Rb^+ ions of overexchanged $Na_{10.4}Rb_{56}Al_{56.1}Si_{135.8}O_{384}$, which is close to the composition of the Rb−Y used in our study. At room temperature they found ca. 9 Rb^+ ions per unit cell occupying the large windows, but twice as many were in there at 400 °C.[39] This Rb^+ occupancy could be overestimated due to the overexchange, but the refinement of the cation distribution in an 80% Cs^+-exchanged zeolite Y yielded a very similar result. Nearly half of the sixteen 7.5-Å apertures per unit cell hosted a Cs^+ at room temperature, but three-quarters of them were

(33) The faujasite framework (zeolites X, Y) is based on 6.5 Å wide sodalite cages, which are connected via hexagonal prisms to form 13 Å wide supercages with tetrahedral symmetry. The unit cell includes eight of the latter, which are interconnected through 7.5 Å apertures. The 2.2 Å windows of the sodalite cages are too narrow to be accessible for Se molecules. The cations occupy in that order sites inside the hexagonal prisms (site I), inside the sodalite cages (sites I′, II′), inside the supercages (site II), and within the large supercage windows (site III).

(34) Hollemann, A. F.; Wiberg, N.; Wiberg, E. *Lehrbuch der Anorganischen Chemie*; deGruyter: Berlin, 1985.

(35) Wachhold, M.; Sheldrick, W. S. *Z. Naturforsch.* **1997**, *52b*, 169.

(36) Sheldrick, W. S.; Wachhold, M. *J. Chem. Soc., Chem. Commun.* **1996**, 607.

(37) Sheldrick, W. S.; Wachhold, M. *Angew. Chem., Int. Ed. Engl.* **1995**, *34*, 450.

(38) Marra, G. L.; Fitch, A. N.; Zecchina, A.; Ricchiardi, G.; Salvalaggio, M.; Bordiga, S.; Lamberti, C. *J. Phys. Chem. B* **1997** *101*, 10653.

(39) Ciraolo, M. F.; Hanson, J. C.; Grey, C. P. *Microporous Mesoporous Mater.* **2001**, *49*, 111.

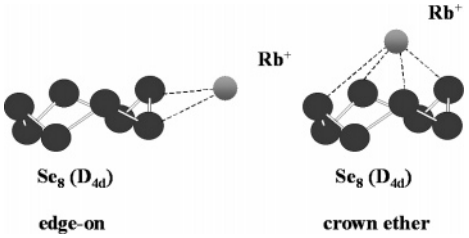

Figure 7. Rb^+ ions coordinated to Se_8 rings in an edge-on (left) and a crown ether-like fashion (right).

occupied by an ion at 350 °C.[40] Thus, 1.5−2 site III Rb^+ ions per supercage will be available for Se_8 coordination at the Se sorption temperature (350 °C). Following the temperature dependence of the ion distribution between sites II and III, the coordination of Rb^+ to Se rings may become less favorable with respect to coordination to the framework at type II sites at lower temperatures. A number of complexes would decompose then upon cooling, leaving behind a mixture of uncomplexed and cation-coordinated Se rings at room temperature.

The above considerations suggest that the not yet assigned Raman bands of the Rb−Y·10Se composite may originate from such an Rb^+/Se_8 complex. Crown ether-like coordinated $[Rb(Se_8)]^+$, $[Rb(Se_8)_2]^+$, and $[Rb_2(Se_8)]^{2+}$ clusters or Se_8 rings edge-on coordinated to one or several Rb^+ ions can be easily accommodated within the supercages (Figure 7). Unfortunately characteristic properties of these clusters are not known, and we are unable at this point to make an unequivocal identification of the species in question based on the Raman spectrum. However, it is useful to discuss how strong complexation of an Se_8 ring by an Rb^+ ion anchored in the zeolite supercage would be manifested in the vibrational spectrum. Since the rings will lose their freedom to rotate and reorient easily in the supercage, localization at a site will be accompanied by the appearance of new librational modes. The lowering of the molecular symmetry will also result in the lifting of degeneracies of vibrational modes, and new internal modes involving the cation displacement will appear. This has been established by recent ab initio quantum chemical calculations on the C_{4v} complexation of Se_8 by Na^+, which also indicate a general weak softening of the Se_8 internal vibrational modes with respect to the uncomplexed ring.[41] Most significantly, a strong new Raman band should arise from the splitting of the degenerate Se_8 mode at 75 cm^{-1} (additional blue-shifted band around 90 cm^{-1}) and a new cation-related mode is predicted around 160 cm^{-1} for this weakly coordinated Na^+ complex.[41] Similar consequences can be expected of the probably stronger complexation of Se_8 by Rb^+ ions. Thus, the Rb−Y·10Se bands at 48, 64, and 98 cm^{-1} could arise from hindered rotations or lifted degeneracies of Se_8, the one at 136 cm^{-1} could be due to a Rb^+-related mode, and the strong bands at 250 and 263 cm^{-1} could be red-shifted due to Rb^+ coordination of Se_8 inside the zeolite cages. However, not all vibrational modes are resolved in Figure 1, and weak shoulders at 43 and 112 cm^{-1} and the broadened band at 79 cm^{-1} suggest that clusters with differing cation coordination could exist.

The proposed combination of complexed and uncomplexed Se_8 clusters is consistent with the excitation wavelength dependence of the Raman spectrum as well. With Se being photosensitive, Rb^+/Se_8 complexes could be increasingly destabilized by photoexcitation at higher energies and decompose into the constituents. Thus, only the ratio between the two clusters is expected to change, which corresponds with the observed relative intensity changes in the Raman spectra. Note that a selective photoinduced break-up of Se_8 or other ring clusters is not very probable, since we have no evidence for degradation products. Such fragments were readily observed when we studied the photoinduced break-up of Se chains encapsulated in zeolite Y.[42,43] Hence, a mixture of Rb^+-coordinated and uncoordinated Se_8 clusters provides a plausible rationale for the complex Raman spectrum displayed in Figure 1. The coordination clusters also enhance the stability of the material, since a significant amount of Se_8 rings will be immobilized within the aluminosilicate framework. This could be the essential reason for the unusual durability of this composite.

Conclusion

We have synthesized a Se/faujasite nanocomposite, Rb−Y·10Se, which exhibits a significantly improved stability in air. The confined selenium has a direct optical band gap of 2.62 eV, which is blue-shifted by more than 0.5 eV with respect to those of amorphous and trigonal Se. The Raman spectrum is neither compatible with long disordered Se chains nor can it be assigned to a single Se ring cluster. The excitation wavelength dependence of the spectrum allows a grouping of the observed modes. The bands at 31, 79, 109, 130, 259, and 272 cm^{-1} are in good agreement with previously calculated Raman modes of Se_8 (D_{4d}) crowns. The remaining modes at 48, 64, 98, 136, 250, 263, and further unresolved shoulders are attributed to stable Rb^+/Se_8 complexes similar to those recently found in crystalline polyselenides. A detailed structural description of these complexes cannot be given yet, but the observed Raman modes are consistent with the general trends expected for cation/Se ring complexes confined in nanoporous aluminosilicates.

The improved stability of this nanocomposite stems from the tendency of Se_8 rings to form strongly bound complexes with Rb^+ cations inside the zeolite supercage. This shifts the equilibrium between Se chains and rings nearly completely toward Se_8. It also immobilizes a large fraction of the Se_8, which impedes the already slow intercage diffusion of uncomplexed rings at room temperature further. Although desirable, an identification of these coordination clusters inside zeolite pores by direct means such as crystallography may prove futile, because of the disordered nature of these composites. Instead, element-sensitive probes such as anomalous X-ray scattering (AXS) and solid-state NMR are currently being used to investigate alkali ion coordination

(40) Norby, P.; Poshni, F. I.; Gualtieri, A. F.; Hanson, J. C.; Grey, C. P. *J. Phys. Chem. B* **1998**, *102*, 839.
(41) Curtiss, L. A. Private communication.
(42) Goldbach, A.; Iton, L.; Grimsditch, M.; Saboungi, M.-L. *J. Am. Chem. Soc.* **1996**, *118*, 2004.
(43) Goldbach, A.; Iton, L.; Grimsditch, M.; Saboungi, M.-L. *J. Phys. Chem. B* **1997**, *101*, 330.

complexes with selenium in zeolite Y. These methods have been previously employed to characterize selenium–cation correlations in zeolites (AXS)[15,16] and the Rb^+–Se_8 interaction in a layered polyselenide (NMR).[44] Quantum chemical calculations are another promising approach to obtain a better insight into the nature of these complexes.

(44) Goldbach, A.; Fayon, F., Vosegaard, T.; Wachhold, M.; Kanartzidis, M. G.; Massiot, D.; Saboungi, M.-L. *Inorg. Chem.* **2003**, *42*, 6996.

Acknowledgment. Work at the Centre de Recherche sur la Matière Divisée was supported by the Centre National de Recherche Scientifique (SPM) and the work at Argonne National Laboratory by the Department of Energy, The Office of Science, under Contract W-31-109-ENG-38. A.G. acknowledges the Region Centre for a special research fellowship. The authors thank L. A. Curtiss for making his unpublished calculations available.

CM049030H